Single stage transmission type broadband solar concentrator

Chih-Ming Wang,[1,*] Hung-I Huang,[2,3] J. W. Pan,[3] Hung-Zen Kuo,[4] Hwen-Fen Hong,[4] Hwa-Yuh Shin,[4] and Jenq-Yang Chang[2,*]

[1]*Institute of Opto-electronic Engineering, National Dong Hwa University, Hualien 97401, Taiwan.*
[2]*Department of Optics and Photonics, National Central University, Jhongli 32001, Taiwan*
[3]*Institute of Photonic System, National Chiao Tung University, Tainan 71150, Taiwan*
[4]*Institute of Nuclear Energy Research, Atomic Energy Council, Executive Yuan 32546, Taiwan*
jychang@dop.ncu.edu.tw

Abstract: In this paper, a single stage solar cell concentrator is designed and discussed. The proposed concentrator consists of refraction prisms and total internal reflection prisms in the inner and outer areas, respectively. In order to compensate for dispersion, all odd zones gather the light onto the – *D* position, while all even zones gather the light onto the + *D* position. Finally, the hybrid concentrator achieves optical efficiency of 89.8% for normally incident light without an antireflection coating. An acceptance angle of ± 0.78° at 1dB loss is achieved without using additional secondary optics. In addition, the fabrication tolerance is also analyzed.

OCIS codes: (220.1770) Concentrator; (260.2030) Dispersion; (220.0220) Optical design and fabrication.

References and links

1. R. King, "Raising the efficiency ceiling with multijunction III-V concentrator photovoltaics," Proceeding 23rd EPVSEC (2008).
2. I. Garca, C. Algora, I. Rey-Stolle, and B. Galiana, "Study of non-uniform light profiles on high concentration III-V solar cells using quasi-3D distributed models," Proceeding 33rd IEEE Photovoltaic Specialist Conference (2008).
3. E. A. Katz, J. M. Gordon, and D. Feuermann, "Effects of ultra-high flux and intensity distribution in multi-junction solar cells," Prog. Photovoltaics **14**(4), 297–303 (2006).
4. R. Winston, and J. M. Gordon, "Planar concentrators near the étendue limit," Opt. Lett. **30**(19), 2617–2619 (2005).
5. W. J. Smith, "Modern Optical Engineer" fourth edition, p.154–155 (Graw Hill 2008)
6. M. Victoria, C. Domínguez, I. Antón, and G. Sala, "Comparative analysis of different secondary optical elements for aspheric primary lenses," Opt. Express **17**(8), 6487–6492 (2009).
7. Breault Research Organization, *http://www.breault.com*.
8. A. Suzuki, and R. Leutz, *Nonimaging Fresnel Lenses: Design And Performance Of Solar Concentrators*, Springer (2006)
9. R. R. King, D. C. Law, K. M. Edmondson, C. M. Fetzer, G. S. Kinsey, H. Yoon, R. A. Sherif, and N. H. Karam, "40% efficient metamorphic GaInP/GaInAs/Ge multijunction solar cells," Appl. Phys. Lett. **90**(18), 183516 (2007).
10. S. N. Kasarova, N. G. Sultanova, C. D. Ivanov, and I. D. Nikolov, "Analysis of the dispersion of optical plastic materials," Opt. Mater. **29**(11), 1481–1490 (2007).
11. D. Vázquez-Moliní, A. Á. Fernández-Balbuena, E. Bernabeu, J. M. L. Clemente, A. Domingo-Manrique, and Á. García-Botella, "New concentrator multifocal Fresnel lens for improved uniformity: design and characterization," Proc. SPIE **7407**, 740701 (2009).

1. Introduction

Multi-junction solar cells are made up of two or more layers of semiconductor materials with different band gaps. Each of these layers is responsible for absorbing light within a particular wavelength range. Therefore, the overall conversion efficiency of a multi-junction solar cell is much higher than that of a single-junction cell. Currently, a III-V-based multi-junction cell can reach efficiencies exceeding 40% [1]. Combining the multi-junction cell with a high solar concentration (above 500 suns) concentrator is a very promising way to reduce the production cost. The concept behind the concentrator photovoltaic (CPV) system is to concentrate light

#125953 - $15.00 USD Received 24 Mar 2010; accepted 3 May 2010; published 19 May 2010

by using low-cost optical elements so that the final product can be as cost-effective as possible. Owing to the fact that plastic-based optical elements can be easily duplicated, a transmission-type concentrator is more cost-effective than a reflective (mirror) one.

Unfortunately, the transmission type CPV suffers from chromatic aberrations due to the nature of the dispersion of the optical material. A typical multi-junction cell, such as an InGaP/InGaAs/Ge multi-junction cell, absorbs solar light over a wide spectral range, from 400nm to 1600nm. Over such a wide spectral range, transmission-type concentrators suffer from a huge dispersion rate. Thus, the optical design of a broadband concentrator with a high concentration range is much more challenging than the design of systems for single-junction solar cells. Moreover, this broadband spectral range makes illuminating the cell with uniform irradiance a challenge. The dispersion can cause either a local hot spot or a blurred spot larger than the cell area. A local hot spot limits the conversion efficiency and may even damage the cell [2,3]. A blurred spot leads to huge energy lose because the irradiance distribution expands out of the cell area. Alternatives to eliminate chromatic aberration include applying an achromatic doublet and/or a diffraction element into the optical system. However, these solutions, respectively, suffer from being too bulky or having a low diffraction efficiency. Alternatively, to eliminate spherical, comatic and chromatic aberration, a reflection-type, aplanatic planar imaging concentrator consisting of two mirrored surfaces, based on the Cassegrain arrangement, has been proposed [4]. This idea works well for the ideal case; however, the tolerance range for the alignment of the two mirrors system is narrow, owing to the fact that any misalignment will be magnified by the two-mirror system [5]. Therefore, this solution suffers from problems relating to accuracy in mass production. Another issue for the CPV system is the acceptance angle of the CPV. Wider acceptance angles allow less stiff trackers, which lead to less material-intensive trackers and, as consequence, cheaper ones. In addition, the alignment tolerance between the concentrator and the tracker also can be reduced.

Conventionally, secondary optics is applied to compensate for the limitations of the primary optics, including the uniformity and angle tolerance [6] mentioned above. However, secondary optics adds reflection loss and cost.

In this study, in order to achieve further energy savings, a single stage solar cell concentrator is designed and discussed. The proposed transmission-type concentrator consists of refraction prisms and total internal reflection prisms in the inner and outer areas, respectively. In order to compensate for dispersion, a focus-complement concentrator is proposed to optimize the uniformity of the solar cell concentrator. Consequently, an irradiance distribution of more uniformity through a spectral range from 400nm to 1600nm is achieved.

In addition to describing the concentrator itself, its optical properties, such as optical efficiency, acceptance angle and fabrication tolerance, will also be discussed.

2. Design and simulation

Figure 1 shows a schematic cross-section of the structure of the proposed concentrator. It is formed by a series of concentric prisms with varying basic angles. The pitch between the prisms is equal and denoted by P. In the inner area of the concentrator, the light is gathered by using refraction. Meanwhile, in the outer area, the light is gathered by using the total internal reflection (TIR). The prism in the inner-most area of the concentrator is called the 1st zone. The outer-most outer is called the 40th zone. In order to compensate for dispersion, all odd zones gather light onto the $-D$ position of the cell while all even zones gather light onto the $+D$ position, respective to the number of zones. The center of the solar cell is defined as $D = 0$. It can be seen that the long wavelength light refracted by the even zones is deflected onto the outer area of the solar chip, while the long wavelength light refracted by the odd zones is deflected onto the inner area of the solar chip. Consequently, the dispersion of the prisms that focus on the $+/-D$ positions is complementary. The optical performance of the concentrator is simulated by using the Advanced System Analysis Program (ASAP), which is a non-sequential ray-tracing method [7].

#125953 - $15.00 USD Received 24 Mar 2010; accepted 3 May 2010; published 19 May 2010

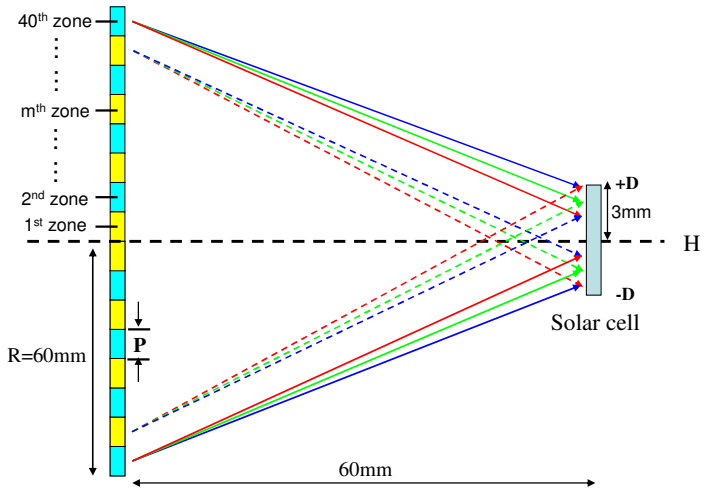

Fig. 1. Schematic representation of the proposed solar concentrator. The inner and outer areas of the concentrator are formed by refraction and TIR prisms, respectively.

The concentrator discussed in this paper is formed by using a series of prisms with variation of the basic angle θ, where θ is $\angle BAC$, as shown in Fig. 2. These concentrically arranged prisms form a Fresnel-type concentrator [8]. The working distance between the concentrator and the solar cell is 60mm and the radius of the concentrator is 60mm. Thus, the deflected angle is from 0° to 45°, and the feature size of the prism is 1.5mm. In such a geometric scale, the diffraction effect can be ignored. Therefore, the optical properties of the concentrator are dominated by the refraction and reflection. Based on the difference in θ, the prism can be divided into two classes: refraction and TIR types. Figure 2(a) shows the deflected angle ϕ as a function of θ. The incident angle is normal and the refractive index of the prism is n = 1.5. The deflected angle increases with an increasing θ. In this regime ($\theta<\theta_C$, where θ_C is the critical angle of the light passing through PMMA to air), the function of the prism is of the refraction type, as shown in Fig. 2(b). For $\theta_C<\theta<(\theta_C + 90)/2$, the incident light is under the TIR condition. At this point, the incident light is reflected by the AB surface, then refracted by the AC surface, as shown in Fig. 2(c), and therefore the deflected angle decreases with an increasing θ.

Given a simple geometric relation, one can calculate the relation between the basic angle, θ, and the deflected angle, ϕ, for the refraction and TIR regimes, respectively:

$$n\sin\theta = \sin(\phi + \theta), \tag{1}$$

$$n\sin(2\theta - 90^o) = \sin(90^o - \phi), \tag{2}$$

where n is the refractive index of the prism. In this study, the prism material is polymethylmethacrylate (PMMA), which is a typical optical plastic with a refractive index from 1.5 to 1.48 for a wavelength from 400 to 1600nm. It can be found that $\partial\phi/\partial\theta > 0$ for the refraction type, while $\partial\phi/\partial\theta < 0$ for the TIR type. This characteristic reveals that the deflection angles for the refraction and TIR types are complimentary.

#125953 - $15.00 USD Received 24 Mar 2010; accepted 3 May 2010; published 19 May 2010

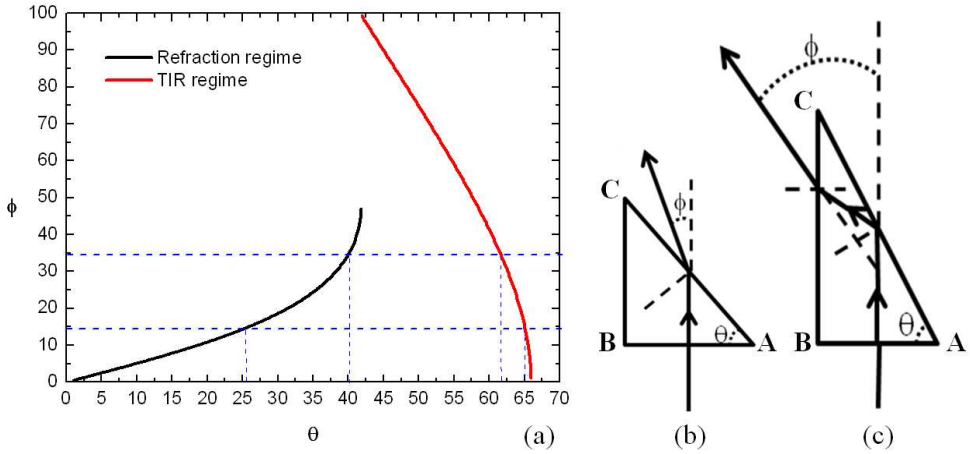

Fig. 2. (a) Deflected angle ϕ as a function of the prism angle θ, where the black and red lines correspond to: the (b) refraction prism; and (c) TIR prism, respectively.

The structure of the concentrator consists of two parts, with the reflection and TIR regimes corresponding to the inner and outer parts, respectively. For a small deflected angle from $0°<\phi<25°$, the corresponding θ can be either $0°<\theta<35°$ for a refraction prism or $62°<\theta<66°$ for a TIR prism. Clearly, although the TIR prism can also deflect the solar light with a small deflected angle, the tolerance of θ is too small for practical fabrication purposes. In addition, at this time, optical efficiency is limited by the Fresnel loss for such a large incident angle. Therefore, for a small deflected angle (i.e. the inner area of the concentrator), it is more appropriate to gather solar light using refraction prisms. For a large deflected angle from $25°<\phi<45°$, the incident angle for the refraction prism is approaching an angle even larger than the critical angle $\theta_C = 41.8°$ for n = 1.5. Thus, the optical efficiency is limited by the Fresnel loss if a refraction prism is applied. Therefore, for a large deflected angle (i.e. the outer area of the concentrator), it is more appropriate to gather solar light using TIR prisms. As is shown in Table 1, from the 1st to the 19th zones of the concentrator, the refraction regime is most appropriate, while from the 20th to 40th, the TIR regime works better. The basic angle of the refraction regime is from $0°<\theta<35°$ while that of the TIR regime is from $59°<\theta<63°$. Light impinges the prism suffers from the Fresnel reflection loss twice. For normally incident condition, the overall Fresnel loss is sum of one normally incident reflection loss and one off-normally incident loss. For n = 1.5 and $\theta = 17°$, the overall Fresnel loss of unpolarized light is 8.1% (4% + 4.1%). For n = 1.5 and $\theta = 61°$, the overall Fresnel loss of unpolarized light is 9.2% (4% + 5.2%). In fact, the refractive index of PMMA is smaller than 1.5 in most conditions. Therefore, the reflection loss can be even lower.

Table 1. Specifications of Concentric Prisms

	Number of Concentric Prisms	Basic Angle	Deflected Angle	Fresnel Loss (Unpolarized)
Refraction regime	1st–19th	$0°<\theta<35°$	$0°<\phi<25°$	$8%<R<13%$
TIR regime	20th–40th	$59°<\theta<63°$	$25°<\phi<45°$	$9%<R<10%$

3. Dispersion and uniformity

Multi-junction cells are made up of two or more layers of semiconductor material with different bandgaps. Each of these layers is responsible for the absorption of light in some particular spectral range. Here, we choose a multi-junction solar cell as a merit target. It is a three-layer solar cell consisting of three active regimes: InGaP, InGaAs and Ge layers [9]. The corresponding spectral ranges of absorption are about 400nm~700nm, 700nm~900nm and 900~1600nm, respectively. Within the spectral range from 400nm to 1600nm, the

#125953 - $15.00 USD Received 24 Mar 2010; accepted 3 May 2010; published 19 May 2010

corresponding refraction index of PMMA is 1.5-1.48, which can be calculated using Cauchy's equation [10]:

$$n^2(\lambda) = A_1 + A_2\lambda^2 + A_3\lambda^{-2} + A_4\lambda^{-4} + \cdots, \quad (3)$$

where A_1 = 2.1875, A_2 = 1.5830 × 10^{-3}, A_3 = 4.8439 × 10^{-3}, A_4 = 2.1192 × 10^{-3}, and A_5 = –2.0907 × 10^{-4} and the unit of λ is μm.

Figure 3 below shows the irradiance distribution on the cell position for PMMA. The refractive index from left to right is 1.48, 1.49 and 1.5, respectively. It has been mentioned that the zones do not gather the light on the center of the solar cell but rather slightly off center, with a distance of *D*. The irradiance distribution for n = 1.49 is discussed first. Figure 3(b) and 3(e) show the irradiance distribution for which the zones gather light in the + *D* and – *D* positions, respectively. These two pictures present an almost identical pattern, a donut shape with an inner and outer radius of 0.7mm and 2.3mm, respectively. Here, the inner and outer radii are defined as the distance between the chip center and the position where the irradiance distribution become 10% of the maximum. The effects of the dispersion under the same geometric parameters are investigated. The donut-shaped distribution becomes a small hot spot when n = 1.48(Fig. 3(a)); it becomes a larger donut when n = 1.5 (Fig. 3(c)). On the other hand, when the zones gather the light on the *–D* position, the donut-shaped distribution becomes a larger donut for n = 1.48 (Fig. 3(d)), whereas it becomes a small hot spot for n = 1.5 (Fig. 3(f)). Conventionally, the primary optics of a concentrator plays the simple role of focusing the light as shown in Fig. 3(a). However, as the index becomes lower (i.e., the wavelength becomes longer), the focused spot becomes blurred. Once the distribution of the irradiance is larger than the entrance of the secondary optics, the optical efficiency is limited. Nevertheless, it can be seen that the irradiance distribution is complementary when the light is focused on the + *D* and *–D* positions. Therefore, when the zones simultaneously gather the light on both + *D* and *–D*, it is straightforward to compensate for the dispersion-induced irradiance distribution change.

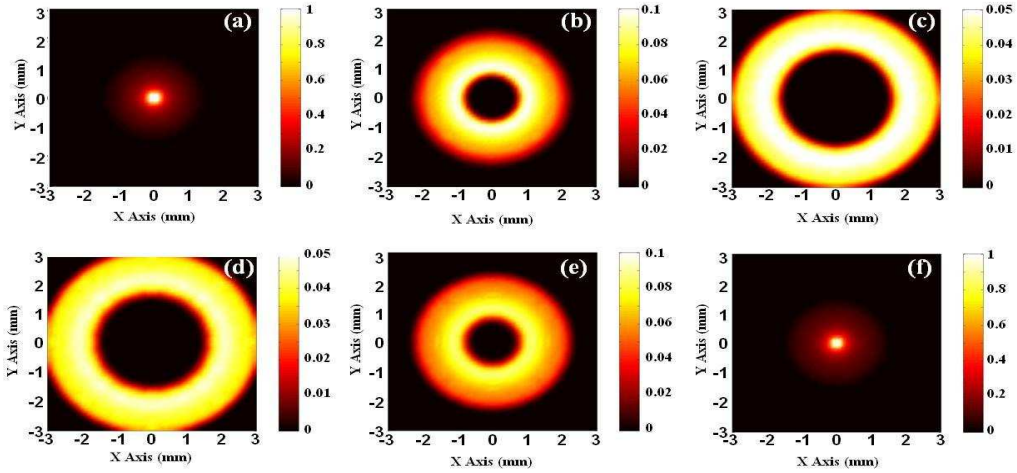

Fig. 3. Irradiance distribution at the solar cell position when the light is focused on the + *D* position and the index of the prism is (a) n = 1.48, (b) n = 1.49 and (c) n = 1.5. When the light is focused on the *–D* position, the irradiance distributions for (d) n = 1.48, (e) n = 1.49 and (f) n = 1.5 are also shown. When the light is focused on the + *D* position with a donut-shaped distribution as shown in 3(b), the light is over-focused or blurred for lower and higher indices, respectively. On the contrary, when the light is focused on the *–D* position with a donut-shaped distribution as shown in 3(e), the light is blurred or over-focused for lower and higher indices, respectively.

In order to compensate for dispersion, the odd zones gather the light onto the *–D* position while the even zones gather the light onto the + *D* position, according to the number of the

#125953 - $15.00 USD Received 24 Mar 2010; accepted 3 May 2010; published 19 May 2010

zones. The irradiance distribution for each absorption layer of the multi-junction cell is simulated. An AM1.5 solar spectrum from 400nm to 1600nm with a wavelength spacing of 2nm is considered. The irradiance distribution shown in Fig. 4 is calculated by the superposition of each absorption layer with the product of the solar spectrum and the irradiance distribution. The light distributions for the spectral range of absorption of the InGaP, InGaAs and Ge layers are shown in Figs. 4(a), 4(b), 4(c), respectively. It can be seen that the simulated irradiance distribution for each layer is uniform and without any hot spots. The irradiance distributions of the three layers are similar. This similarity is advantageous given the design of the current-matching in multi-junction cells. In addition, most of the light is focused within the cell area. The efficiencies for the InGaP, InGaAs and Ge layers are η = 39.9%, η = 22.1% and η = 27.8%, respectively. The optical efficiency η is defined by the ratio of the power reaching the cell divided by the incoming solar power from 400nm to 1600nm. Finally, the overall optical efficiency for the AM1.5 solar spectrum from 400nm to 1600nm is η = 89.8%, without applying an additional anti-reflection coating.

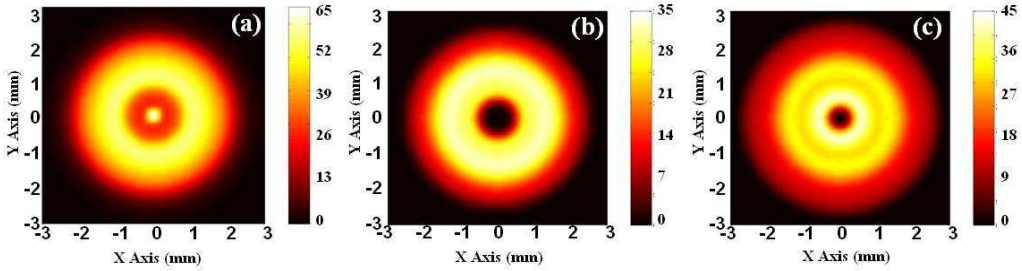

Fig. 4. Irradiance distributions at the solar cell position for the absorption spectral range of (a) InGaP layer (400nm~700nm), (b) InGaAs layer (700nm~900nm), and (c) Ge layer (900nm~1600) when the odd zones gather the light on to the + *D* position and the even zones gather the light on to the –*D* position.

4. Acceptance angle and fabrication tolerance

The acceptance angle of the concentrator influences the requirements of the tracker stiffness enormously. When the acceptance angle is narrow, alignment and assembly difficulties arise. The simulated efficiency as a function of the deviation angle from the normal incident direction of the proposed concentrator is shown in Fig. 5. The input solar light is assumed to be AM1.5. The black line indicates the overall optical efficiency as a function of the incident angle. As shown in Fig. 5, the optical efficiency is η = 89.8% for normally incident light. It has to be mentioned that the shape of the prism is assumed to be a right angle prism. As the prism is not a perfect right angle, the effective cross-section of the prism becomes small [8,11]. Practically, the optical loss due to the decreased effective cross-section is about 8%. In addition, in this paper, the vertex and the valleys of the prisms are assumed to be a sharp corner. Practically, the optical loss due to the rounded corners is about 3% [11]. Both of the loss due to the rounded corners and the decreased effective cross-section is not considered. It can be seen that overall optical efficiency decreases slightly as the deviation angle increases from 0° to 0.5°. The acceptance angle, $\alpha_{90\%}$, of the proposed concentrator is ± 0.78°, which is not too demanding for a conventional solar tracker. Here, $\alpha_{90\%}$ is defined as the deviation angle where optical efficiency becomes 90% of the maximum. The red, green and blue dashed lines indicate the optical efficiency for the InGaP, InGaAs and Ge layers, respectively. The $\alpha_{90\%}$ for InGaP, InGaAs and Ge layers is 0.77°, 0.79° and 0.73°, respectively. Regarding that the sun is a disc-like source but not a point source. Therefore, parts of the solar light impinge the concentrator with a varying angle even when the tracker is well aligned. Nevertheless, the angular diameter of the sun is 0.53° at the surface of the earth which is smaller than the acceptance angle. This means that the proposed concentrator is sufficient to gather the light emitting from the edge of sun.

#125953 - $15.00 USD Received 24 Mar 2010; accepted 3 May 2010; published 19 May 2010

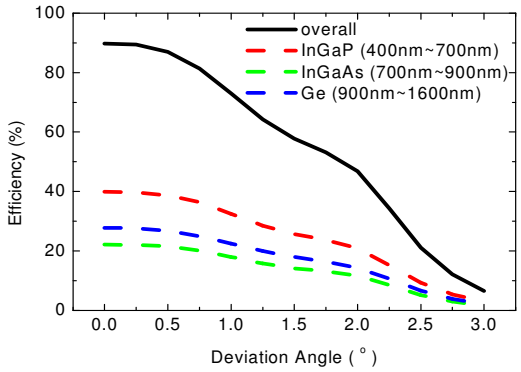

Fig. 5. Acceptance angle of the proposed concentrator. The black solid line indicates the overall efficiency. The red, green and blue dashed lines indicate the optical efficiency for InGaP, InGaAs and Ge layers, respectively. The input solar light is assumed to be AM1.5. $\alpha_{90\%}$, of the overall efficiency is ± 0.78°.

Here, we consider a concentric prism with an equal pitch of 1.5mm, which is much larger than the practical fabrication tolerance. Therefore, the tolerance of the pitch is ignorable. The fabrication tolerance is dominated by the basic angle θ of the prisms. We assume that the basic angle is $\theta_{ideal} + \Delta\theta$, the sum of the ideal basic angle θ_{ideal}, and the fabrication error $\Delta\theta$. Thus, $\Delta\theta$ is defined as the standard deviation of a Gaussian normal distribution:

$$p(x) = \frac{1}{\sqrt{2\pi\sigma^2}} \exp\left(-\frac{x^2}{2\sigma^2}\right), \ \sigma = \Delta\theta \tag{4}$$

where $p(x)$ is the probability density function. Figure 6 shows that the optical efficiency depends on the fabrication error. It can be seen that with a fabrication error as large as 0.5°, the optical efficiency drops to 90% of the ideal case. This fabrication tolerance is also not too demanding for practical manufacturing. As mentioned before, owing that the deflection angles of the refraction- and TIR-type prisms are complimentary for a varying basic angle, the fabrication tolerance can be thus improved.

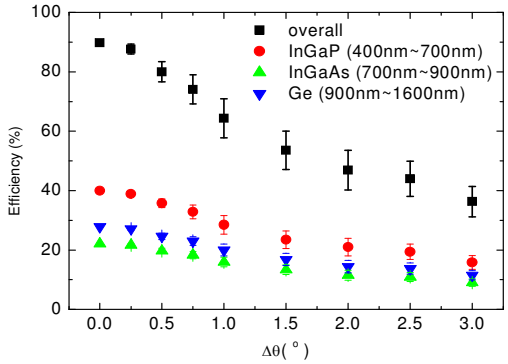

Fig. 6. Optical efficiency as a function of the fabrication error, $\Delta\theta$. The black color indicates the overall optical efficiency. The red, green and blue colors indicate the optical efficiencies for the InGaP, InGaAs and Ge layers, respectively.

#125953 - $15.00 USD Received 24 Mar 2010; accepted 3 May 2010; published 19 May 2010

5. Conclusion

In this paper, a single stage solar cell concentrator intended to increase energy savings is designed and discussed. The proposed transmission-type concentrator consists of refraction prisms and total internal reflection prisms in the inner and outer areas, respectively. In order to compensate for dispersion, the odd zones gather the light onto the $-D$ position while the even zones gather the light onto the $+D$ position, according to the number of zones. Consequently, an irradiance distribution of improved uniformity through the spectral range from 400nm to 1600nm is achieved. The hybrid concentrator presents 89.8% efficiency for normally incident light without an antireflection coating. An acceptance angle $\theta_{90\%} = \pm 0.78°$ is achieved without the use of an additional secondary optics. In addition, the fabrication tolerance is also analyzed.

Acknowledgements

The authors are grateful for the financial support received for this study from the Institute of Nuclear Energy Research, Atomic Energy Council of Taiwan under project number 982001INER033.

#125953 - $15.00 USD Received 24 Mar 2010; accepted 3 May 2010; published 19 May 2010